

## THE X-RAY HALO OF THE LOCAL GROUP AND THE CMB QUADRUPOLE

Yasushi SUTO

*Research Center for the Early Universe, School of Science,  
The University of Tokyo, Tokyo 113, JAPAN*

### Abstract

Since recent X-ray observations have revealed that most clusters of galaxies are surrounded by an X-ray emitting gaseous halo, it is reasonable to expect that the Local Group of galaxies has its own X-ray halo. We show that such a halo, with temperature  $\sim 1\text{keV}$  and column density  $\sim O(10^{21})\text{cm}^{-2}$ , is a possible source for the excess low-energy component in the X-ray background. The halo should also generate temperature anisotropies in the microwave background via the Sunyaev-Zel'dovich effect. Assuming an isothermal spherical halo with the above temperature and density, the amplitude of the induced quadrupole turns out to be comparable to the COBE data without violating the upper limit on the  $y$ -parameter.

### 1. Introduction

The origin of the X-ray background (XRB) remains one of the most challenging problems in X-ray astrophysics. Figure 1 summarizes the current results on the XRB energy spectra,  $I(\varepsilon)$  below 10 keV observed with different satellites. As is known (McCammon & Sanders 1990; Fabian & Barcons 1992),  $I(\varepsilon) \sim 10\varepsilon^{-0.4}\text{keV} \cdot \text{s}^{-1} \cdot \text{sr}^{-1} \cdot \text{keV}^{-1}$  is a good empirical fit over the range 3 to 10 keV, where  $\varepsilon$  denotes X-ray energy in units of keV. In the soft band, however, the observed spectra do not seem to be in perfect agreement among different satellites; both Einstein IPC (Wu et al. 1991; plotted in diamonds) and ROSAT (Hasinger 1992; Shanks et al. 1991; upper-left lines) data suggest a large excess below 2 keV. More recently the Japanese X-ray satellite ASCA (crosses) reported a modest but significant excess soft component below 1 keV relative to the extrapolation of the above power-law fit in the higher energy band (Gendreau et al. 1995). Thus the existence of the soft excess is well established although its amplitude is still somewhat controversial.

Since Galactic absorption becomes important in the soft X-ray energy band, the origin of this excess component allows several possibilities including Galactic sources, extragalactic point-like sources (Hasinger 1992; Shanks et al. 1991), a diffuse thermal component (Wang & MaCray 1993), the accumulation of the thermal bremsstrahlung emission from the low temper-

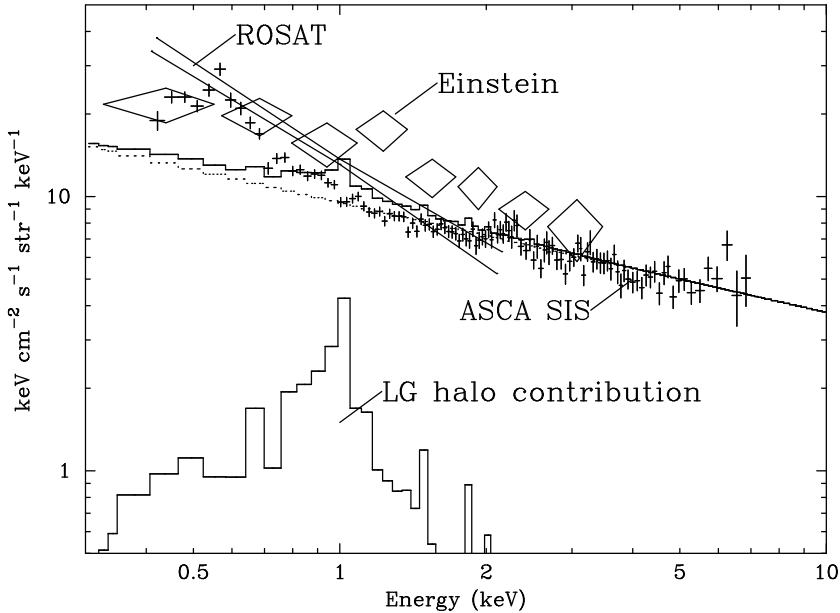


Fig. 1. XRB spectra observed with different X-ray satellites and expected contribution from the halo of the Local Group (Suto et al. 1996).

ature low-density plasma surrounding distant clusters of galaxies (Cen et al. 1995; Kitayama & Suto 1996). Figure 2 shows an example of theoretical predictions of the contribution of clusters on the XRB in the standard cold dark matter model ( $\Omega_0 = 1$ ,  $\lambda_0 = 0$ ,  $\Omega_b = 0.06$ ,  $h = 0.5$ ) which is normalized by COBE (Sugiyama 1995). Here  $\Omega_0$ ,  $\lambda_0$ ,  $\Omega_b$ , and  $h$  are the cosmological density parameter, the dimensionless cosmological constant, the baryon density parameter, and the Hubble constant in units of 100km/s/Mpc. Three lines indicate the theoretical predictions on the basis of the Press-Schechter theory but with different assumption on the cluster evolution (Kitayama & Suto 1996 for details). Also plotted are the observed data from *ASCA* with statistical errors (Gendreau et al. 1995), and the simulation by Kang et al. (1994; triangles). This suggests that the clusters of galaxies can in fact account for the observed soft-excess in the XRB.

## 2. Sunyaev-Zel'dovich effect due to the halo of the Local Group

Yet another possibility which we propose here is the emission from an X-ray halo of the Local Group (LG). Since the gaseous halos of clusters of galaxies are known to be strong sources of X-rays, it is reasonable to assume that the LG has its own X-ray halo. To be more specific, suppose that the LG is associated with a spherical isothermal plasma whose electron number density is given by

$$n_e(r) = n_0 \frac{r_c^2}{r^2 + r_c^2}, \quad (1)$$

where  $n_0$  is the central density and  $r_c$  is the core radius. If we are located at distance  $x_0$  off the LG center (Fig. 3), the electron column density at angular separation  $\theta$  from the direction to the center is

$$N_e(\mu) = \int_0^\infty \frac{n_0 r_c^2 d\xi}{\xi^2 - 2x_0\mu\xi + x_0^2 + r_c^2} = \frac{n_0 r_c^2}{x_0} \frac{1}{\sqrt{a^2 - \mu^2}} \left[ \frac{\pi}{2} + \sin^{-1} \left( \frac{\mu}{a} \right) \right], \quad (2)$$

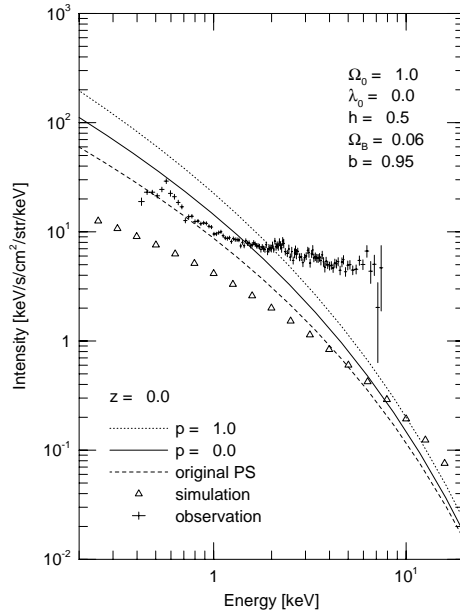


Fig. 2. The XRB spectra contributed from clusters of galaxies (Kitayama & Suto 1996).

where  $\mu \equiv \cos \theta$ , and  $a \equiv \sqrt{1 + (r_c/x_0)^2}$ .

In Fig. 1 the LG halo contribution to the XRB spectra simulated with the Raymond-Smith model assuming an isothermal plasma temperature  $T = 1\text{keV}$ ,  $r_c = 0.15\text{Mpc}$ ,  $x_0 = 0$ ,  $n_0 = 10^{-4}\text{cm}^{-3}$  and 0.3 times solar abundances is also plotted (lower-left histogram). This LG halo model has a total X-ray luminosity of  $10^{41}\text{erg} \cdot \text{s}^{-1}$  between 0.5keV and 4keV, and an electron column density of  $6 \times 10^{20}\text{cm}^{-2}$ . If we add this component to  $I(\varepsilon) = 9.6\varepsilon^{-0.4}\text{keV} \cdot \text{s}^{-1} \cdot \text{sr}^{-1} \cdot \text{keV}^{-1}$ , the soft excess around 1 keV is explained (solid line). Note that it is not our primary purpose here to find the best fit parameters because the single power-law component is simply an extrapolation from the higher energy band and also because the possible Galactic absorption is not taken into account here. Nevertheless it is interesting to see that the LG halo can be a possible origin for the soft excess.

If the X-ray halo of the LG really exists and accounts for the soft excess component in the XRB, it should also produce temperature anisotropies in the cosmic microwave background (CMB) via the Sunyaev-Zel'dovich (SZ) effect (Zel'dovich & Sunyaev 1969; Cole & Kaiser 1988; Makino & Suto 1993; Persi et al. 1995). In the Rayleigh-Jeans regime, the SZ temperature decrement is given by

$$\left(\frac{\delta T}{T}\right)_{sz}(\mu) = -2\frac{kT}{mc^2}\sigma_T N_e(\mu), \quad (3)$$

where  $k$  is the Boltzmann constant,  $m$  is the electron mass,  $c$  is the velocity of light, and  $\sigma_T$  is the cross section of the Thomson scattering. We compute the multipoles expanded in spherical harmonics:

$$\left(\frac{\delta T}{T}\right)(\theta, \varphi) = \sum_{l=0}^{\infty} \sum_{m=-l}^l a_l^m Y_l^m(\theta, \varphi). \quad (4)$$

With eqs.(2) and (4), one obtains

$$(a_l^0)_{sz} = -2\sqrt{(2l+1)\pi}\frac{kT}{mc^2}\sigma_T \int_{-1}^1 N_e(\mu)P_l(\mu) d\mu, \quad (5)$$



Fig. 3. Geometry of the X-ray halo of the Local Group.

where  $P_l(\mu)$  are the Legendre polynomials. Averaging over the sky, the above SZ anisotropies are expected to contribute in quadrature to the CMB anisotropies as

$$\left\langle \left( \frac{\delta T}{T} \right)^2 \right\rangle = \frac{1}{4\pi} \sum_{l=0}^{\infty} (2l+1) \langle |a_l^m|^2 \rangle = \frac{1}{4\pi} \sum_{l=0}^{\infty} (a_l^0)_{sz}^2 \equiv \sum_{l=0}^{\infty} (T_{l,sz})^2. \quad (6)$$

The corresponding monopole, dipole and quadrupole anisotropies reduce to

$$T_{0,sz} = \pi \theta_c \sigma_T \frac{kT}{mc^2} \frac{n_0 r_c^2}{x_0}, \quad (7)$$

$$T_{1,sz} = 2\sqrt{3} \left( 1 - \frac{r_c}{x_0} \theta_c \right) \sigma_T \frac{kT}{mc^2} \frac{n_0 r_c^2}{x_0}, \quad (8)$$

$$T_{2,sz} = \frac{\sqrt{5}\pi}{4} \left[ \theta_c - 3 \frac{r_c}{x_0} + 3 \left( \frac{r_c}{x_0} \right)^2 \theta_c \right] \sigma_T \frac{kT}{mc^2} \frac{n_0 r_c^2}{x_0}, \quad (9)$$

where  $\theta_c \equiv \tan^{-1}(x_0/r_c)$ .

The *COBE* FIRAS data (Mather et al. 1994) imply that the Compton  $y$ -parameter,  $y$ , should be less than  $2.5 \times 10^{-5}$  (95% confidence level). With eq.(7), this upper limit is translated to

$$n_0 r_c^2 / x_0 < 1.1 \times 10^{22} \left( \frac{1.17}{\theta_c} \right) \left( \frac{y}{2.5 \times 10^{-5}} \right) \left( \frac{1 \text{keV}}{T} \right) \text{cm}^{-2}. \quad (10)$$

For example taking  $r_c = 0.15 \text{Mpc}$  and  $x_0 = 0.35 \text{Mpc}$ , the constraint (10) indicates that

$$T_{1,sz} < 3 \times 10^{-5} \left( \frac{y}{2.5 \times 10^{-5}} \right), \quad (11)$$

$$T_{2,sz} < 1.3 \times 10^{-5} \left( \frac{y}{2.5 \times 10^{-5}} \right). \quad (12)$$

The analysis of the 1st 2 years' *COBE* DMR data (Bennett et al. 1994; Wright et al. 1994), on the other hand, yields  $T_{1,\text{COBE}} = (1.23 \pm 0.09) \times 10^{-3}$ , and  $T_{2,\text{COBE}} = (2.2 \pm 1.1) \times 10^{-6}$ . Therefore the LG X-ray halo can potentially have significant effect on the quadrupole of the CMB anisotropies, while its effect on dipole is totally negligible compared to the peculiar velocity of the LG with respect to the CMB rest frame.

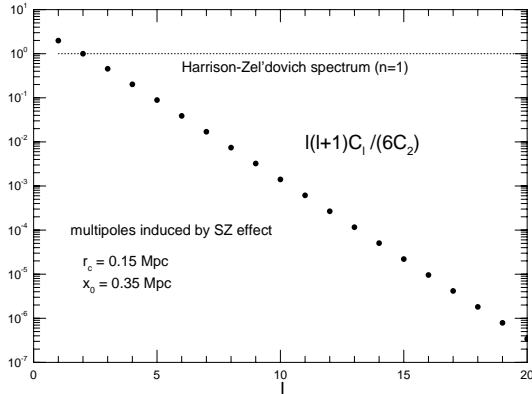


Fig. 4. Multipoles induced by the Sunyaev-Zel'dovich effect of the Local Group halo (Suto et al. 1996). The primordial Harrison-Zel'dovich spectrum prediction  $l(l+1)C_l/(6C_2) = 1$  is plotted in dotted line.

### 3. Implications for the CMB temperature anisotropies

Primordial density fluctuations with power spectrum  $P(k) \propto k^n$  induce CMB anisotropies via the Sachs-Wolfe effect with multipoles (e.g., Peebles 1993)

$$C_l \equiv \langle |a_l^m|^2 \rangle \propto \frac{\Gamma(l + n/2 - 1/2)}{\Gamma(l - n/2 + 5/2)}, \quad (13)$$

where  $\Gamma(\nu)$  is the Gamma function. Therefore the standard Harrison-Zel'dovich ( $n = 1$ ) spectrum predicts that

$$\frac{l(l+1)C_l}{6C_2} = 1. \quad (14)$$

The analytic expressions for the higher multipoles (eq.[5]) are quite complicated. Instead we have numerically computed  $(C_l)_{sz} \equiv (a_l^0)_{sz}^2 / (2l+1)$  which are plotted in Fig. 4. Clearly the higher multipoles decrease very rapidly with  $l$ . Thus even if the CMB quadrupole were contaminated by the SZ effect described here, the higher moments would be relatively free from such an effect and can be interpreted to reflect the true cosmological signature (the octapole may be affected to some extent).

Although the contribution of a distant cluster of galaxies to the multipoles is small, its cumulative effect over the high-redshift may be observable in the small-scale CMB anisotropies (Bennett et al. 1993; Makino & Suto 1993; Persi et al. 1995). Figure 5 shows such examples in cold dark matter (CDM) and primeval isocurvature baryon (PIB; Peebles 1987; Sugimoto & Suto 1992) models together with the observational upper limit from the triple beam switching experiment at Owens Valley Radio Observatory (Readhead et al. 1989). The temperature anisotropies predicted in CDM models with  $n = 1$  are below the current observational limit, while PIB models are compatible with the limit only for the  $n = -1$  models with  $\Omega_0 \lesssim 0.1$ ,  $\lambda_0 = 1 - \Omega_0$ , and  $h = 0.5$  (Makino & Suto 1993 for details). The  $n = 0$  PIB models have too much small-scale power leading to the larger SZ temperature fluctuations than the  $n = -1$  models.

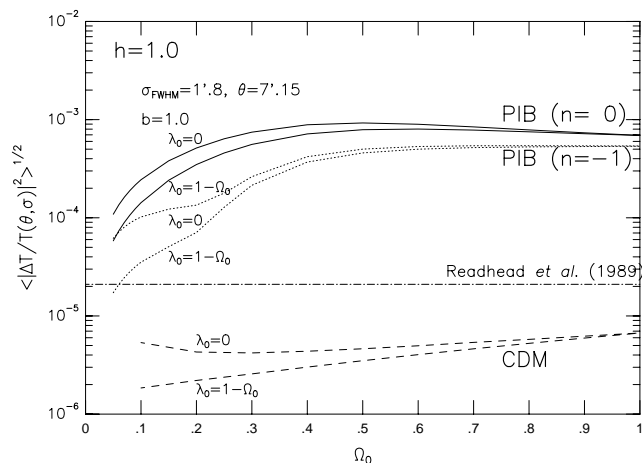


Fig. 5. Small-scale temperature anisotropies in the CMB due to the SZ effect of distant clusters of galaxies (Makino & Suto 1993).

Incidentally it is interesting to note that the *rms* quadrupole amplitude from the *COBE* 2 years' data,  $Q_{\text{rms}} = (6 \pm 3)\mu\text{K}$ , is significantly smaller than that expected from the higher multipoles (Bennett et al. 1994; Wright et al. 1994); if one fixes  $n = 1$ , for instance, the power spectrum fitting using eq.(13) requires that the most likely amplitude should be  $Q_{\text{rms-PS}} = (18.2 \pm 1.5)\mu\text{K}$ . It is somewhat common to ascribe the difference to cosmic variance. It is possible, however, to account for it in terms of our model described here, depending on the actual pattern of the primordial temperature fluctuations.

#### 4. Discussion

The above argument can be used in putting constraints on the properties of the possible LG halo from the *COBE* data. As summarized in Fig. 6, however, the parameter range which is required for the LG halo to provide the excess soft component is largely consistent with the current *COBE* data. In addition, the LG X-ray halo should produce a dipole signature (toward M31 and the opposite direction) in the soft excess component; the flux  $f$  plotted in Fig. 1 corresponds to what should be observed at the center of the halo. If we adopt  $x_0 = 0.35\text{Mpc}$ , the flux towards M31 should be  $1.27f$  while  $0.73f$  for the opposite direction. Such a level of XRB variation is detectable with careful data analysis of, for instance, the *ASCA* GIS observation.

Our model described above assumes a fairly idealistic density profile (1). A more realistic profile of the halo including non-sphericity and spatial inhomogeneity in temperature and density will have a stronger effect on the higher multipoles ( $l \geq 3$ ). Therefore one might even probe the properties of the LG halo through the multipoles of the CMB map. The direct X-ray detection of, or constraints on, the LG halo component is of great importance in deriving the primordial spectral index  $n$  and the amplitude of the density fluctuations from the *COBE* data.

The present work is based on my collaboration with Yoshitaka Ishisaki, Tetsu Kitayama, Nobuyoshi Makino, Kazuo Makishima, and Yasushi Ogasaka. This research was supported in part by the Grants-in-Aid by the Ministry of Education, Science and Culture of Japan (07740183, 07CE2002).

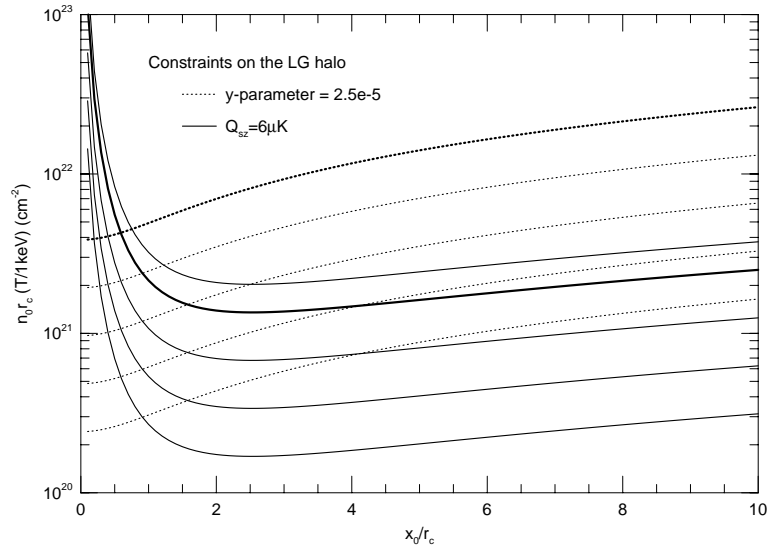


Fig. 6. Constraints on the density and the size of the halo of the Local Group from CMB anisotropies (Suto et al. 1996). Dotted curves correspond to  $y = 2.5 \times 10^{-5}$  (thick),  $2.5 \times 10^{-5}/2$ ,  $2.5 \times 10^{-5}/4$ ,  $2.5 \times 10^{-5}/8$ , and  $2.5 \times 10^{-5}/16$ . Solid curves correspond to  $Q_{sz} = 9\mu\text{K}$ ,  $6\mu\text{K}$  (thick),  $3\mu\text{K}$ ,  $1.5\mu\text{K}$ , and  $0.75\mu\text{K}$ .

1. Bennett, C.L. et al. 1993, *ApJL*, **414**, L77.
2. Bennett, C.L. et al. 1994, *ApJ*, **436**, 423.
3. Cen, R., Kang, H., Ostriker, J.P., & Ryu, D. 1995, *ApJ*, **451**, 436.
4. Cole, S. & Kaiser, N. 1988, *MNRAS*, **233**, 637.
5. Fabian, A.C. & Barcons, X. 1992, *ARA & A*, **30**, 543.
6. Gendreau, K.C. et al 1995, *Pub. Astron. Soc. Japan.*, **47**, L5.
7. Hasinger, G. 1992, *The X-ray Background* eds. Barcons, X. & Fabian, A.C., (Cambridge University Press: Cambridge), 229.
8. Kitayama, T. & Suto, Y. 1996, *MNRAS*, in press.
9. Makino, N. & Suto, Y. 1993, *ApJ*, **405**, 1.
10. Mather, J.C. et al. 1994, *ApJ*, **420**, 439.
11. McCammon, D. & Sanders, W.T. 1990, *ARA & A*, **28**, 657.
12. Peebles, P. J. E. 1987, *ApJ*, **315**, L73.
13. Peebles, P.J.E. 1993, *Principles of Physical Cosmology* (Princeton University Press: Princeton)
14. Persi, F.M., Spergel, D.N., Cen, R., & Ostriker, J.P. 1995, *ApJ*, **442**, 1.
15. Readhead, A. C. S., Lawrence, C. R., Myers, S. T., Sargent, W. L. W., Hardebeck, H. E., & Moffet, A. T. 1989, *ApJ*, **346**, 566.
16. Shanks, T. et al. 1991, *Nature*, **353**, 315.
17. Sugihara, T. & Suto, Y. 1992, *ApJ*, **387**, 431.
18. Sugiyama, N. 1995, *ApJS*, **100**, 281.
19. Suto, Y., Makishima, K., Ishisaki, Y., & Ogasaka, Y. 1996, *ApJL*, in press.
20. Wang, Q.D., & MaCray, R. 1993, *ApJ*, **409**, L37.
21. Wright, E.L., Smoot, G.F., Bennett, C.L., & Lubin, P.M. 1994, *ApJ*, **436**, 443.
22. Wu, X., Hamilton, T., Helfand, D.J., & Wang, Q. 1991, *ApJ*, **379**, 564.
23. Zel'dovich, Ya.B. & Sunyaev, R.A. 1969, *Ap.Sp.Sci.*, **4**, 301.